Observational Constraints on Exponential Gravity

Louis Yang,* Chung-Chi Lee,† Ling-Wei Luo,‡ and Chao-Qiang Geng§

Department of Physics, National Tsing Hua University, Hsinchu 300, Taiwan

(Dated: October 12, 2010)

Abstract

We study the observational constraints on the exponential gravity model of $f(R) = -\beta R_s(1 - e^{-R/R_s})$. We use the latest observational data including Supernova Cosmology Project (SCP) Union2 compilation, Two-Degree Field Galaxy Redshift Survey (2dFGRS), Sloan Digital Sky Survey Data Release 7 (SDSS DR7) and Seven-Year Wilkinson Microwave Anisotropy Probe (WMAP7) in our analysis. From these observations, we obtain a lower bound on the model parameter β at 1.27 (95% CL) but no appreciable upper bound. The constraint on the present matter density parameter is $0.245 < \Omega_m^0 < 0.311$ (95% CL). We also find out the best-fit value of model parameters on several cases.

PACS numbers: 98.80.-k, 04.50.Kd, 95.36.-x

* louis.lineage@msa.hinet.net

† g9522545@oz.nthu.edu.tw

‡ d9622508@oz.nthu.edu.tw

§ geng@phys.nthu.edu.tw

I. INTRODUCTION

Cosmic observations from type Ia supernovae (SNe Ia) [1, 2], large scale structure (LSS) [3, 4], baryon acoustic oscillations (BAO) [5] and cosmic microwave background (CMB) [6, 7] indicate that our universe is undergoing an accelerating expansion. The reason for this acceleration, the so-called dark energy problem, remains a fascinating question today. The simplest model to explain this problem is the ΛCDM model, in which a time independent energy density is added to the universe. However, the ΛCDM model suffers from both fine-tuning and coincidence problems [8–13]. In general, the ways to understand the cosmic acceleration can be separated into two branches. One is to modify the matter by introducing some kind of "dark energy". The other one is to modify Einstein's general relativity – the modification of gravity.

In modified gravity, one of the popular approaches is to promote the Ricci scalar R in the Einstein-Hibert action to a function, $f(R)$. Although there are several viable $f(R)$ models, many of them are restricted to the regimes to be effectively identical to the ΛCDM by the observational constraints. Recently, Linder [14] has explored an $f(R)$ theory named "exponential gravity", which has also been discussed in Refs. [15–17]. The exponential gravity has the feature that it allows the relaxation of fine-tuning and it has only one more parameter than the ΛCDM model. In addition, the exponential gravity satisfies all conditions for the viability [18] such as the local gravity constraint, stability of the late-time de Sitter point, constraints from the violation of the equivalence principle, stability of cosmological perturbations, positivity of the effective gravitational coupling, and asymptotic behavior to the ΛCDM model in the high curvature regime. In this paper, we will study the constraints given by latest observational data, reexamine the alleviation of the fine-tuning problem, and find the possibility of the derivation from ΛCDM. We use units of $k_{\rm B} = c = \hbar = 1$ and the gravitational constant is given by $G = M_{\rm Pl}^{-2}$ with the Planck mass of $M_{\rm Pl} = 1.2 \times 10^{19}$ GeV.

The paper is organized as follows. In Sec. II, we review equations of motion and the asymptotic behavior at the high redshift regime in the exponential gravity model. In Sec. III, we discuss the observations and methods. We show our results in Sec. IV. Finally, conclusions are given in Sec. V.

II. EXPONENTIAL GRAVITY

The action of $f(R)$ gravity with matter is given by

$$S = \frac{1}{2\kappa^2} \int d^4x \sqrt{-g} \left[R + f(R) \right] + S_m, \tag{2.1}$$

where $\kappa^2 \equiv 8\pi G$ and $f(R)$ is a function of the Ricci scalar curvature R. In this paper, we focus on the exponential gravity model [14], given by

$$f(R) = -\beta R_s (1 - e^{-R/R_s}), \tag{2.2}$$

where R_s is related to the characteristic curvature modification scale. Since the product of β and R_s can be determined by the present matter density Ω_m^0 [14], we can choose β and Ω_m^0 as the free parameters in the model.

We use the standard metric formalism. From the action (2.1), the modified Friedmann equation of motion becomes [19]

$$H^2 = \frac{\kappa^2 \rho_M}{3} + \frac{1}{6}(f_R R - f) - H^2 \left(f_R + f_{RR} R' \right), \tag{2.3}$$

where $H \equiv \dot{a}/a$ is the Hubble parameter, a subscript R denotes the derivative with respect to R, a prime represents $d/d\ln a$, and $\rho_M = \rho_m + \rho_r$ is the energy density of all perfect fluids of generic matter including (non-relativistic) matter, denoted by m, and relativistic particles, denoted by r. Here, we only consider the matter density. Since the modification by the exponential gravity only happens at the low redshift, the contributions from relativistic particles are negligible. In a flat spacetime, the Ricci scalar is given by

$$R = 12H^2 + 6HH'.$$

Following Hu and Sawicki's parameterization [20], we define

$$y_H \equiv \frac{\rho_{DE}}{\rho_m^0} = \frac{H^2}{m^2} - a^{-3}, \quad y_R \equiv \frac{R}{m^2} - 3a^{-3}, \tag{2.4}$$

where $m^2 \equiv \kappa^2 \rho_m^0/3$, ρ_{DE} is the effective dark energy density, and ρ_m^0 is the present matter density. Then, Eqs. (2.3) and (2.4) can be rewritten as two coupled differential equations,

$$y_H' = \frac{y_R}{3} - 4y_H \tag{2.5}$$

and

$$y'_R = 9a^{-3} - \frac{1}{H^2 f_{RR}}\left[y_H + f_R\left(\frac{H^2}{m^2} - \frac{R}{6m^2}\right) + \frac{f}{6m^2}\right], \tag{2.6}$$

where R and H^2 can be further replaced by y_R and y_H from equations in (2.4). Combining Eqs. (2.5) and (2.6), we obtain a second order differential equation of y_H,

$$y''_H + J_1 y'_H + J_2 y_H + J_3 = 0, \tag{2.7}$$

where

$$\begin{aligned} J_1 &= 4 - \frac{1}{y_H + a^{-3}}\frac{f_R}{6m^2 f_{RR}}, \\ J_2 &= -\frac{1}{y_H + a^{-3}}\frac{f_R - 1}{3m^2 f_{RR}}, \\ J_3 &= -3a^{-3} + \frac{f_R a^{-3} + f/3m^2}{y_H + a^{-3}}\frac{1}{6m^2 f_{RR}}, \end{aligned} \tag{2.8}$$

with

$$R = m^2\left[3\left(y'_H + 4y_H\right) + 3a^{-3}\right]. \tag{2.9}$$

Solving Eq. (2.7) numerically, we can get the evolution of the Hubble parameter in the low redshift regime ($z = 0 \sim 4$). The effective dark energy equation of state w_{DE} is given by

$$w_{DE} = -1 - \frac{y'_H}{3y_H}. \tag{2.10}$$

In the high redshift regime ($z \gtrsim 4$), the exponential factor e^{-R/R_S} of $f(R)$ in Eq. (2.2) becomes negligible ($e^{-R/R_S} < 10^{-5}$). The exponential gravity model behaves essentially like a cosmological constant model with the dark energy density parameter $\Omega_\Lambda = \beta R_S/6H_0^2 \cong \Omega_m^0 y_H(z_{high})$. Thus, the Hubble parameter as a function of z in this regime can be expressed as

$$H(z) = H_0\sqrt{\Omega_m^0\left(1+z\right)^3 + \Omega_r^0\left(1+z\right)^4 + \frac{\beta R_S}{6H_0^2}}, \tag{2.11}$$

where Ω_r^0 is the density parameter of relativistic particles including photons and neutrinos[1]. The equation (2.11) will be used in the data fitting of CMB and the high redshift part of BAO in section III.

---

[1] $\Omega_r^0 = \Omega_\gamma^0\left(1 + 0.2271 N_{eff}\right)$, where Ω_γ^0 is the present fractional photon energy density and $N_{eff} = 3.04$ is the effective number of neutrino species [21].

III. OBSERVATIONAL CONSTRAINTS

To constrain the free parameters of β and Ω_m^0 in the exponential gravity model, we use three kinds of the observational data including SNe Ia, BAO and CMB. The SNe Ia and CMB data lead to constraints at the low and high redshift regimes, respectively, while the BAO data provide constraints at the both regimes.

A. Type Ia Supernovae (SNe Ia)

The observations of SNe Ia, known as "standard candles", give us the information about the luminosity distance D_L as a function of the redshift z. The distance modulus μ is defined as

$$\mu_{th}(z_i) \equiv 5\log_{10} D_L(z_i) + \mu_0, \tag{3.1}$$

where $\mu_0 \equiv 42.38 - 5\log_{10} h$ with $H_0 = h \cdot 100km/s/Mpc$ is the present value of the Hubble parameter. The Hubble-free luminosity distance for the flat universe is

$$D_L(z) = (1+z)\int_0^z \frac{dz'}{E(z')}, \tag{3.2}$$

where $E(z) = H(z)/H_0$. The χ^2 of the SNe Ia data is

$$\chi^2_{SN} = \sum_i \frac{[\mu_{obs}(z_i) - \mu_{th}(z_i)]^2}{\sigma_i^2}, \tag{3.3}$$

where μ_{obs} is the observed value of the distance modulus. Since the absolute magnitude of SNe Ia is unknown, we should minimize χ^2_{SN} with respect to μ_0, which relates to the absolute magnitude, and expand it to be [22, 23]

$$\chi^2_{SN} = A - 2\mu_0 B + \mu_0^2 C, \tag{3.4}$$

where

$$A = \sum_i \frac{[\mu_{obs}(z_i) - \mu_{th}(z_i;\mu_0 = 0)]^2}{\sigma_i^2},$$
$$B = \sum_i \frac{\mu_{obs}(z_i) - \mu_{th}(z_i;\mu_0 = 0)}{\sigma_i^2}, \quad C = \sum_i \frac{1}{\sigma_i^2}. \tag{3.5}$$

The minimum of χ^2_{SN} with respect to μ_0 is

$$\tilde{\chi}^2_{SN} = A - \frac{B^2}{C}. \tag{3.6}$$

We adopt this $\tilde{\chi}^2_{SN}$ for our later χ^2 minimization. We will use the data from the Supernova Cosmology Project (SCP) Union2 compilation, which contains 557 supernovae [24], ranging from $z = 0.015$ to $z = 1.4$.

B. Baryon Acoustic Oscillations (BAO)

The observation of BAO measures the distance ratios of $d_z \equiv r_s(z_d)/D_V(z)$, where D_V is the volume-averaged distance, r_s is the comoving sound horizon and z_d is the redshift at the drag epoch [25]. The volume-averaged distance $D_V(z)$ is defined as [5]

$$D_V(z) \equiv \left[(1+z)^2 D_A^2(z) \frac{z}{H(z)}\right]^{1/3}, \tag{3.7}$$

where $D_A(z)$ is the proper angular diameter distance:

$$D_A(z) = \frac{1}{1+z} \int_0^z \frac{dz'}{H(z')}, \quad \text{(for flat universe)}. \tag{3.8}$$

The comoving sound horizon $r_s(z)$ is given by

$$r_s(z) = \frac{1}{\sqrt{3}} \int_0^{1/(1+z)} \frac{da}{a^2 H(z'=\frac{1}{a}-1) \sqrt{1 + (3\Omega_b^0/4\Omega_\gamma^0)a}}, \tag{3.9}$$

where Ω_b^0 and Ω_γ^0 are the present values of baryon and photon density parameters, respectively. We use $\Omega_b^0 = 0.022765h^{-2}$ and $\Omega_\gamma^0 = 2.469 \times 10^{-5} h^{-2}$ [21]. The fitting formula for z_d is given by [26]

$$z_d = \frac{1291(\Omega_m^0 h^2)^{0.251}}{1 + 0.659(\Omega_m^0 h^2)^{0.828}} \left[1 + b_1(\Omega_b^0 h^2)^{b2}\right], \tag{3.10}$$

where

$$\begin{aligned} b_1 &= 0.313(\Omega_m^0 h^2)^{-0.419} \left[1 + 0.607(\Omega_m^0 h^2)^{0.674}\right], \\ b_2 &= 0.238(\Omega_m^0 h^2)^{0.223}. \end{aligned} \tag{3.11}$$

The typical value of z_d is about 1021 with $\Omega_m^0 = 0.276$ and $h = 0.705$. Since z_d is in the high redshift regime, we use Eq. (2.11) to calculate $r_s(z_d)$. On the other hand, $D_V(z)$ is evaluated by the numerical result of Eq. (2.7) as it is in the low redshift regime.

The BAO data from the Two-Degree Field Galaxy Redshift Survey (2dFGRS) and the Sloan Digital Sky Survey Data Release 7 (SDSS DR7) [25] measured the distance ratio d_z at two redshifts $z = 0.2$ and $z = 0.35$ to be $d^{obs}_{z=0.2} = 0.1905 \pm 0.0061$ and $d^{obs}_{z=0.35} = 0.1097 \pm 0.0036$ with the inverse covariance matrix:

$$C^{-1}_{BAO} = \begin{pmatrix} 30124 & -17227 \\ -17227 & 86977 \end{pmatrix}. \tag{3.12}$$

The χ^2 for the BAO data is

$$\chi^2_{BAO} = (x^{th}_{i,BAO} - x^{obs}_{i,BAO})(C^{-1}_{BAO})_{ij}(x^{th}_{j,BAO} - x^{obs}_{j,BAO}), \tag{3.13}$$

where $x_{i,BAO} \equiv (d_{0.2}, d_{0.35})$.

C. Cosmic Microwave Background (CMB)

The CMB is sensitive to the distance to the decoupling epoch z_* [27]. It can give constraints on the model in the high redshift regime ($z \sim 1000$). The CMB data are taken from Wilkinson Microwave Anisotropy Probe (WMAP) observations [21]. To use the WMAP data, we compare three quantities: (i) the acoustic scale l_A,

$$l_A(z_*) \equiv (1 + z_*)\frac{\pi D_A(z_*)}{r_S(z_*)}, \tag{3.14}$$

(ii) the shift parameter R [28],

$$R(z_*) \equiv \sqrt{\Omega^0_m} H_0(1 + z_*)D_A(z_*), \tag{3.15}$$

and (iii) the redshift of the decoupling epoch z_*. The fitting function of z_* is given by [29]

$$z_* = 1048 \left[1 + 0.00124(\Omega^0_b h^2)^{-0.738}\right] \left[1 + g_1(\Omega^0_m h^2)^{g2}\right], \tag{3.16}$$

where

$$g_1 = \frac{0.0783(\Omega^0_b h^2)^{-0.238}}{1 + 39.5(\Omega^0_b h^2)^{0.763}}, \quad g_2 = \frac{0.560}{1 + 21.1(\Omega^0_b h^2)^{1.81}}. \tag{3.17}$$

The χ^2 of the CMB data is

$$\chi^2_{CMB} = (x^{th}_{i,CMB} - x^{obs}_{i,CMB})(C^{-1}_{CMB})_{ij}(x^{th}_{j,CMB} - x^{obs}_{j,CMB}), \tag{3.18}$$

where $x_{i,CMB} \equiv (l_A(z_*), R(z_*), z_*)$ and C^{-1}_{CMB} is the inverse covariance matrix. The data from Seven-Year Wilkinson Microwave Anisotropy Probe (WMAP7) observations [21] lead to $l_A(z_*) = 302.09$, $R(z_*) = 1.725$ and $z_* = 1091.3$ with the inverse covariance matrix:

$$C^{-1}_{CMB} = \begin{pmatrix} 2.305 & 29.698 & -1.333 \\ 29.698 & 6825.27 & -113.180 \\ -1.333 & -113.180 & 3.414 \end{pmatrix}. \tag{3.19}$$

Finally, the χ^2 of all the observational data is

$$\chi^2 = \tilde{\chi}^2_{SN} + \chi^2_{BAO} + \chi^2_{CMB}. \tag{3.20}$$

In our fitting process, we did not use the Markov chain Monte Carlo (MCMC) approach because the numerical calculation for each solution of $f(R)$ theory is very time-consuming, and the necessary change to the code like CosmoMC [30] is very extensive with no obvious benefit in our study of the exponential gravity. Therefore, we take the simple χ^2 method as our main fitting procedure. The ΛCDM result obtained from SNe Ia, BAO and CMB constraints with this χ^2 method is $\Omega_m^0 = 0.276^{+0.014}_{-0.013}$, while that with the MCMC method is $\Omega_m^0 = 0.272^{+0.013}_{-0.011}$ [31]. We note that the fitting in Ref. [31] has also included the observational constraints from the radial BAO and Hubble parameter H(z).

TABLE I. The best-fit values of the matter density parameter Ω_m^0 (68% CL) and χ^2 for the exponential gravity model with $\beta = 2, 3, 4$ and the ΛCDM model. Note that the error for Ω_m^0 is obtained when β is fixed.

Model		Ω_m^0	χ^2
	$\beta = 2$	$0.274^{+0.014}_{-0.013}$	546.7136
Exponential Gravity	$\beta = 3$	$0.276^{+0.014}_{-0.013}$	545.3836
	$\beta = 4$	$0.276^{+0.014}_{-0.013}$	545.1721
ΛCDM		$0.276^{+0.014}_{-0.013}$	545.1522

IV. RESULTS

Based on the methods described in Sec. III, we now examine the parameter space of the exponential gravity model. In Fig. 1, we present likelihood contour plots at 68.3, 95.4 and 99.7% confidence levels obtained from the SNe Ia, BAO and CMB constraints. The results show that the observational data give no upper bound on the model parameter β, making it a free parameter. Hence, there is no fine-tuning problem. However, a larger value of β, which is closer to the ΛCDM model, is slightly preferred by the observational data as expected. The lower bound on β is $\beta > 1.27$ (95% CL). The present matter density parameter Ω_m^0 is constrained to $0.245 < \Omega_m^0 < 0.311$ (95% CL), which agrees with the

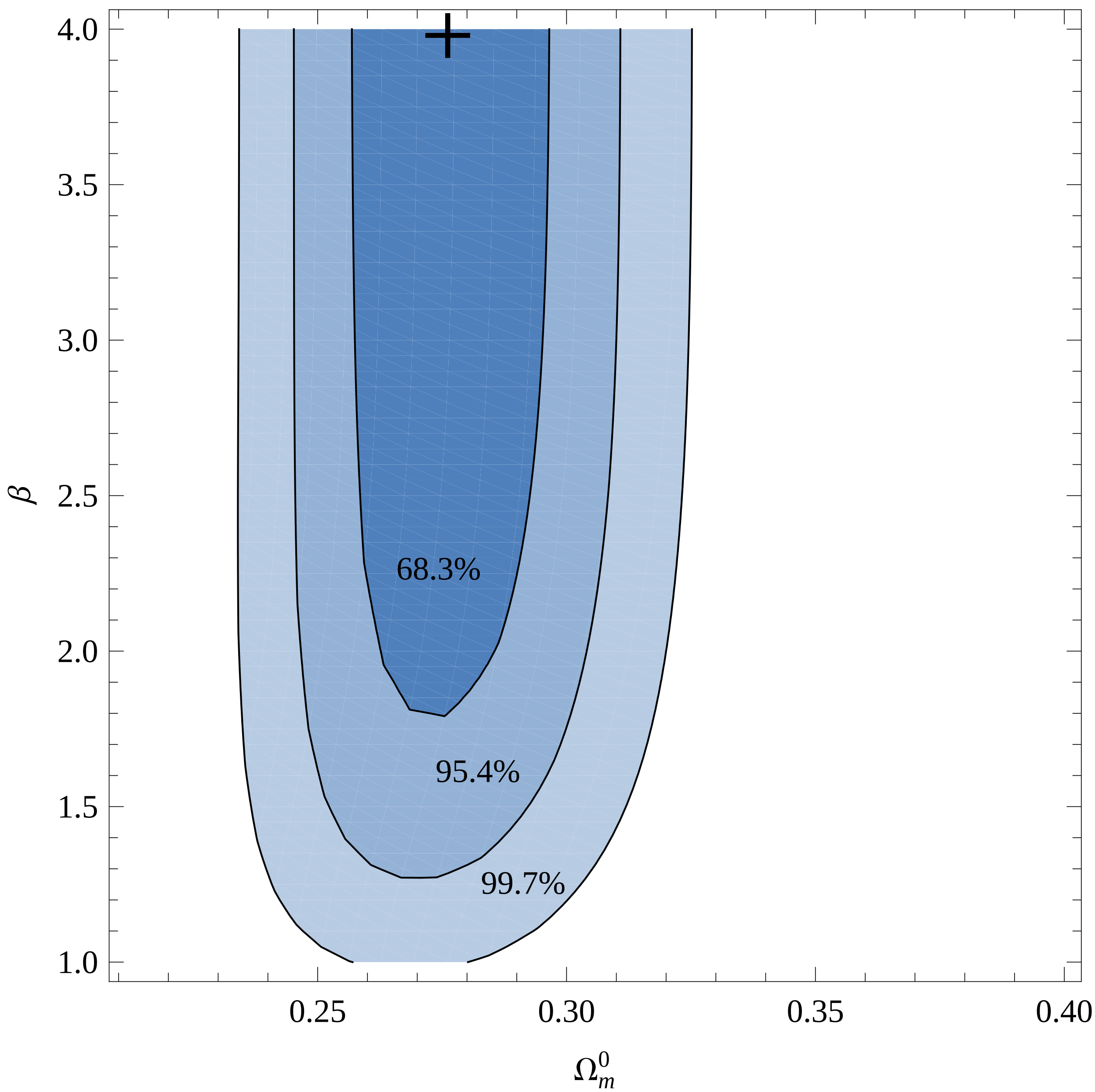

FIG. 1. The 68.3%, 95.4% and 99.7% confidence intervals for the exponential gravity model, constrained by the SNe Ia, BAO, and CMB data. The best-fit point in this parameter region is marked with a plus sign.

current observations. The best-fit value (smallest χ^2) in the parameter space between $\beta = 1$ and 4[2] is $\chi^2 = 545.1721$ with $\beta = 4$ and $\Omega_m^0 = 0.276$. The comparison of the best-fit Ω_m^0 and χ^2 for the model with $\beta = 2, 3, 4$ and ΛCDM is shown in Table I.

[2] We only concentrate on the region of $1 < \beta < 4$. For $\beta > 4$, it is almost the ΛCDM model. For $\beta < 1$, it is ruled out by the local gravity constraints and the stability of the de-Sitter phase.

In Fig. 2, we illustrate the evolution of the effective dark energy equation of state w_{DE} for $\beta = 2, 3, 4$ with their best-fit Ω_m^0, which is given in Table I. We can see that, for every value of β, the effective dark energy equation of state w_{DE} starts at the phase of a cosmological constant $w_{DE} = -1$ and evolves from the phantom phase ($w_{DE} < -1$) to the non-phantom phase ($w_{DE} > -1$). And, for larger value of β, the deviation from cosmological constant phase ($w_{DE} = -1$) become smaller. For $\beta = 2$, there is still another small oscillation after the main phantom phase crossing. Negative z means the future evolution. It is clear that the exponential gravity model has the feature of crossing the phantom phase in the past as well as the future [32].

In Fig. 3, we depict the effective dark energy density Ω_{DE} and non-relativistic matter density Ω_m vs. the redshift z.

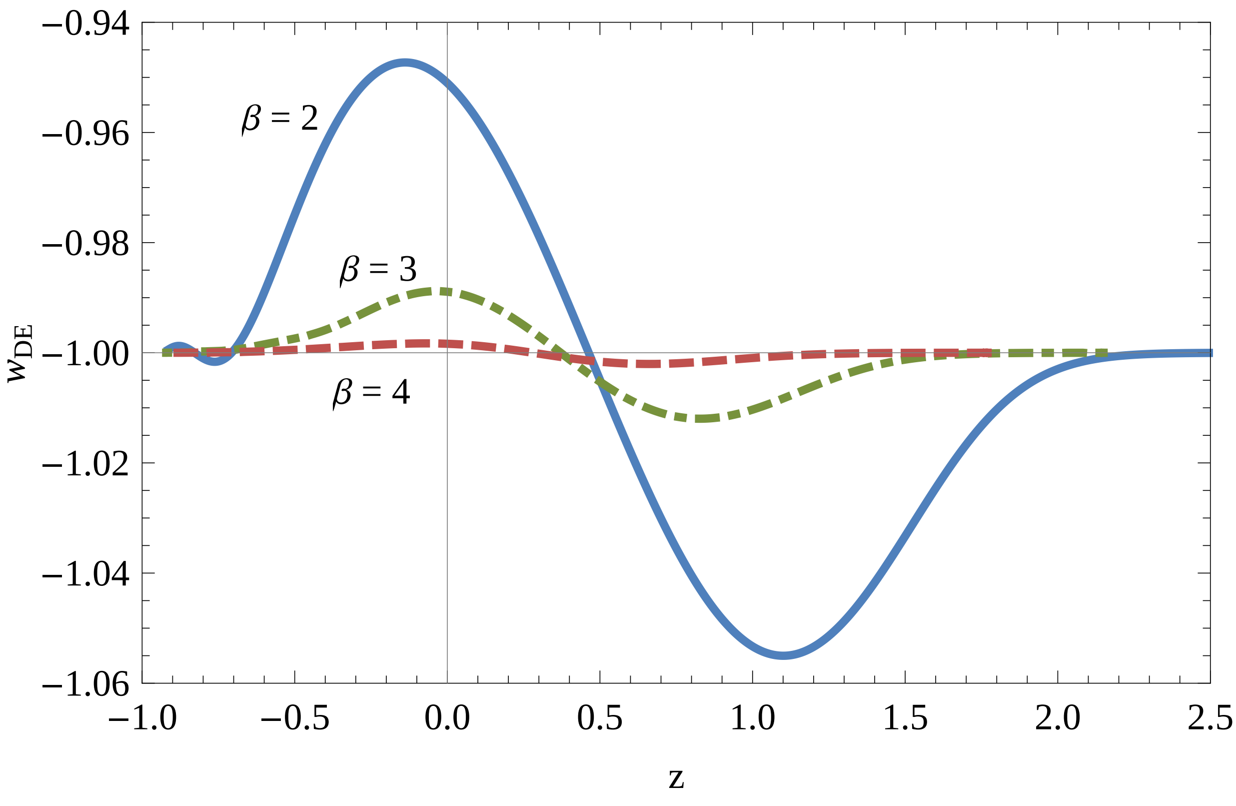

FIG. 2. Evolution of the effective dark energy equation of state w_{DE} corresponding to $\beta = 2, 3, 4$ with their best-fit Ω_m^0 given in Table I.

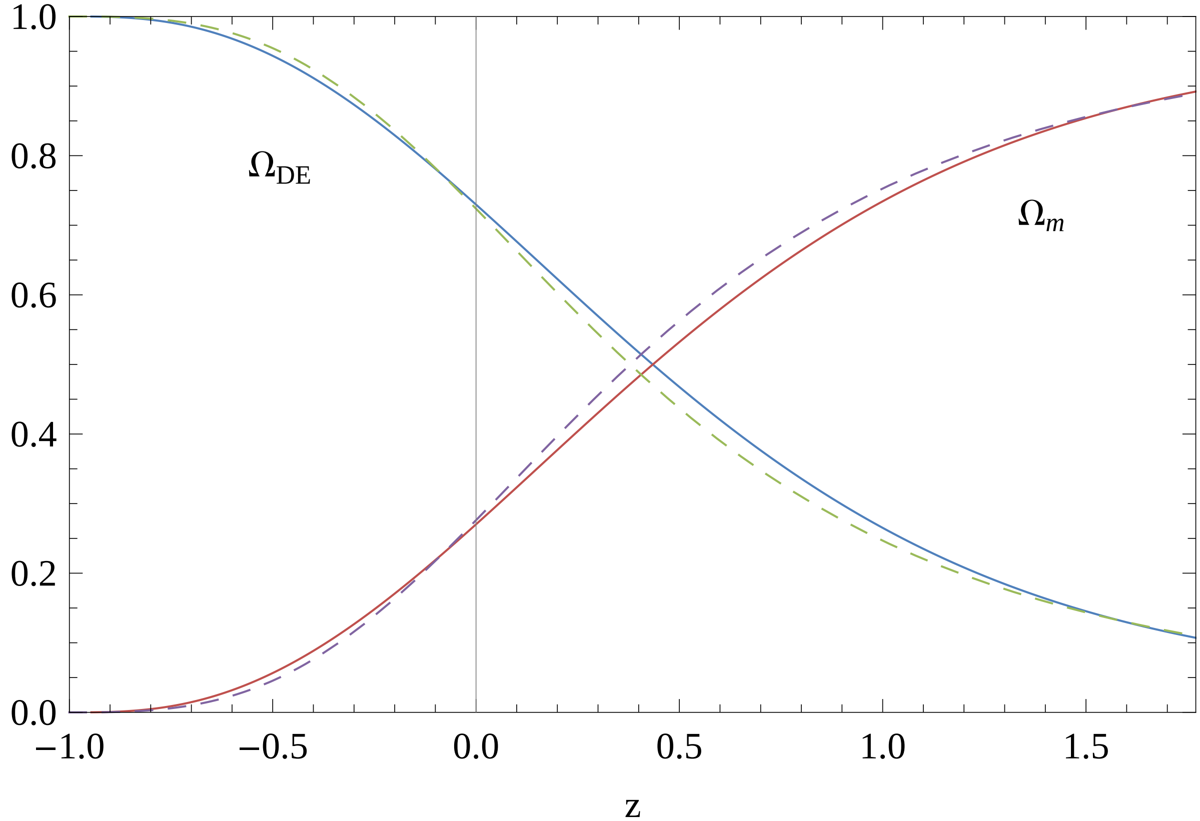

FIG. 3. The evolutions of the effective dark energy density parameter Ω_{DE} and non-relativistic matter density parameter Ω_m as functions of z, where the solid lines indicate the exponential gravity model with $\beta = 1.27$ and the best-fit $\Omega_m^0 = 0.270$ and the dashed lines represent the ΛCDM model with $\Omega_m^0 = 0.276$. For a higher value of β, the evolution becomes closer to that in ΛCDM.

V. CONCLUSION

We have studied the exponential gravity model. In the low redshift regime, we follow Hu and Sawicki's parameterization to form the differential equation for the exponential gravity and solve it numerically. In the high redshift regime, we take advantage of the asymptotic behavior of the exponential gravity toward an effective cosmological constant. The analytical form of the Hubble parameter H as a function of the redshift z can be expressed in the high redshift limit. We have constrained the parameter space of the model by the SNe Ia, BAO and CMB data. We have found that there is a lower bound on the model parameter β at 1.27 but no upper limit, and Ω_m^0 is constrained to the concordance value. This means that the exponential gravity model shows no need of fine-tuning. Nevertheless, the ΛCDM model is still included by the observational constraints since $\beta \to \infty$ corresponds to the model. Current observational data still lack the ability to distinguish between the ΛCDM and exponential gravity models.

Finally, we remark that as seen from Fig. 3, the noticeable difference between the exponential gravity and ΛCDM models lies in the regime $0.2 < z < 1$, and is maximized at $z = 0.5$ if we compare their expected distance modulus. An improvement on the BAO observation may give a stronger constraint on this redshift regime or higher. The ongoing and future dark energy survey projects which will observe BAO include WiggleZ [33], BOSS (Baryon Oscillation Spectroscopic Survay) [34], HETDEX (Hobby-Eberly Dark Energy Experiment) [35], EUCLID [36], JDEM (Joint Dark Energy Mission)/Omega with Wide Field Infrared Survey Telescope (WFIRST) [37], BigBOSS (Big Baryon Oscillation Spec-troscopic Survay) [38], SKA (Square Kilometer Array) [39], LSST (Large Synoptic Survey Telescope) [40] and DES (Dark Energy Survey) [41]. In addition, it is known that the measurement on the growth rate of $f_g(z) = d\ln\delta_m/d\ln a$ has the potential to distinguish the models with the same expansion history but different physics. In the exponential gravity case, the growth index is $\gamma = 0.540$ for $\beta = 2$. It is clear that if those surveys such as WiggleZ, EUCLID, BigBOSS and JDEM/Omega can measure the growth rate with a high accuracy, they will be able to discriminate the exponential gravity from the ΛCDM model.

ACKNOWLEDGMENTS

We thank Dr. K. Bamba for many helpful discussions and suggestions. The work is supported in part by the National Science Council of R.O.C. under: Grant #: NSC-98-2112-M-007-008-MY3 and National Tsing Hua University under the Boost Program #: 97N2309F1.

[1] A. G. Riess *et al.* [SNST Collaboration], Astron. J. **116**, 1009 (1998).

[2] S. Perlmutter *et al.* [SNCP Collaboration], Astrophys. J. **517**, 565 (1999).

[3] M. Tegmark *et al.*, [SDSS Collaboration], Phys. Rev. D **69**, 103501 (2004).

[4] U. Seljak *et al.* [SDSS Collaboration], Phys. Rev. D **71**, 103515 (2005).

[5] D. J. Eisenstein *et al.* [SDSS Collaboration], Astrophys. J. **633**, 560 (2005).

[6] D. N. Spergel *et al.* [WMAP Collaboration], Astrophys. J. Suppl. **148**, 175 (2003).

[7] D. N. Spergel *et al.* [WMAP Collaboration], Astrophys. J. Suppl. **170**, 377 (2007).

[8] S. Weinberg, Rev. Mod. Phys. **61**, 1 (1989).

[9] V. Sahni and A. A. Starobinsky, Int. J. Mod. Phys. D **9**, 373 (2000).

[10] S. M. Carroll, Living Reviews in Relativity **4** (2001).

[11] P. J. E. Peebles and B. Ratra, Rev. Mod. Phys. **75**, 559 (2003).

[12] T. Padmanabhan, Phys. Rept. **380**, 235 (2003).

[13] E. J. Copeland, M. Sami and S. Tsujikawa, Int. J. Mod. Phys. D **15**, 1753 (2006).

[14] E. V. Linder, Phys. Rev. D **80**, 123528 (2009).

[15] P. Zhang, Phys. Rev. D **73**, 123504 (2006).

[16] P. Zhang, M. Liguori, R. Bean, and S. Dodelson, Phys. Rev. Lett. **99**, 141302 (2007).

[17] G. Cognola, E. Elizalde, S. Nojiri, S. D. Odintsov, L. Sebastiani, and S. Zerbini, Phys. Rev. D **77**, 046009 (2008).

[18] K. Bamba, C. Q. Geng and C. C. Lee, JCAP **1008**, 021 (2010) [arXiv:1005.4574 [astro-ph.CO]].

[19] Y. S. Song, W. Hu, and I. Sawicki, Phys. Rev. D **75**, 044004 (2007).

[20] W. Hu and I. Sawicki, Phys. Rev. D 76, 064004 (2007).

[21] E. Komatsu *et al.* [WMAP Collaboration], arXiv:1001.4538 [astro-ph.CO].

[22] S. Nesseris and L. Perivolaropoulos, Phys. Rev. D **72**, 123519 (2005).

[23] L. Perivolaropoulos, Phys. Rev. D **71**, 063503 (2005).

[24] R. Amanullah *et al.*, Astrophys. J. **716**, 712 (2010), arXiv:1004.1711 [astro-ph.CO].

[25] W. J. Percival *et al.*, Mon. Not. Roy. Astron. Soc. **401**, 2148 (2010), arXiv:0907.1660 [astro-ph.CO].

[26] D. J. Eisenstein and W. Hu, Astrophys. J. **496**, 605 (1998), arXiv:astro-ph/9709112.

[27] E. Komatsu *et al.* [WMAP Collaboration], Astrophys. J. Suppl. **180**, 330 (2009), arXiv:0803.0547 [astro-ph].

[28] J. R. Bond, G. Efstathiou, and M. Tegmark, Mon. Not. Roy. Astron. Soc. **291**, L33 (1997), arXiv:astro-ph/9702100.

[29] W. Hu and N. Sugiyama, Astrophys. J. **471**, 542 (1996), arXiv:astro-ph/9510117.

[30] A. Lewis and S. Bridle, Phys. Rev. D **66**, 103511 (2002), arXiv:astro-ph/0205436.

[31] Y. Gong, X. ming Zhu, and Z.-H. Zhu, arXiv:1008.5010 [astro-ph.CO].

[32] K. Bamba, C. Q. Geng and C. C. Lee, arXiv:1007.0482 [astro-ph.CO].

[33] K. Glazebrook *et al.*, ASP conference series **379**, 72 (2007), arXiv:astro-ph/0701876.

[34] D. Schlegel, M. White, and D. Eisenstein [with input from the SDSS-III], arXiv:0902.4680 [astro-ph.CO].

[35] G. J. Hill *et al.*, ASP conference series **399**, 115 (2008), arXiv:0806.0183 [astro-ph].

[36] European Space Agency Euclid Mission, http://sci.esa.int/euclid/.

[37] N. Gehrels, arXiv:1008.4936 [astro-ph.CO]. See also http://jdem.gsfc.nasa.gov/.

[38] D. J. Schlegel *et al.*, arXiv:0904.0468 [astro-ph.CO].

[39] The Square Kilometre Array, http://www.skatelescope.org/.

[40] J. A. Tyson, D. M. Wittman, J. F. Hennawi, and D. N. Spergel, Nucl. Phys. Proc. Suppl. **124**, 21 (2002), arXiv:astro-ph/0209632; J. A. Tyson [LSST Collaboration], Proc. SPIE Int. Soc. Opt. Eng. **4836**, 10 (2002), arXiv:astro-ph/0302102; AIP Conf. Proc. **870**, 44 (2006), arXiv:astro-ph/0609516; see also http://www.lsst.org/.

[41] The Dark Energy Survey, http://www.darkenergysurvey.org/.